Zero-field spin-noise spectrum of an alkali vapor with strong spin-exchange coupling

Ya Wen [1,2] Xiangyu Li,[1,2] Guiying Zhang,[3] and Kaifeng Zhao [1,2,*]

[1]*Key Laboratory of Nuclear Physics and Ion-Beam Application (MOE), Fudan University, Shanghai 200433, China*
[2]*Department of Nuclear Science and Technology, Institute of Modern Physics, Fudan University, Shanghai 200433, China*
[3]*College of Science, Zhejiang University of Technology, Hangzhou 310023, China*

We present a theoretical and experimental paper of the zero-field optical spin noise (OSN) spectrum for a thermal state alkali vapor in the strong spin-exchange coupling regime. We show that the OSN spectrum consists of two components corresponding to a positive and a negative hyperfine spin correlation (HSC). We quantify the power ratio of each HSC component to the total OSN as a function of probe's detuning. At some special detunings, the OSN spectrum contains only one kind of HSC. At far detunings, the negative HSC component holds more power than the positive one for alkali isotopes with nuclear-spin-number $I > 1$. We also briefly discuss the effect of the negative HSC component on spin squeezing experiments.

I. INTRODUCTION

Spin-exchange (SE) between the valence electrons of two alkali atoms [1–4] or between the electron of an alkali atom and the nucleus of a noble gas atom [5–8] plays an important role in the physics of atomic magnetometers [9], atomic clocks [10], magnetic resonance imaging [11,12], precision measurements [13,14], and neutron science [8].

During a spin-exchange collision (SEC), whereas the total spin of the colliding pair is conserved, an individual spin may flip randomly. In a magnetic field, SECs relax the collective transverse spin component if the participants have different g factors or can jump between states of different g factors. However, in the strong SE coupling regime where the SEC rate far exceeds other relaxation rates and the difference of the Larmor frequencies of the participants, all spins are coupled together and precess coherently with no SE relaxation anymore [4,15]. This effect lies at the heart of many applications of quantum metrology, such as the spin-exchange relaxation-free (SERF) magnetometer [16,17], atomic rotation sensors [18,19], searches of new forces [20–22], spin entanglement, and squeezing in ultracold alkali gases [23–28].

Under SECs, whereas ultracold alkali atoms can remain on the lower hyperfine multiplet of the ground state [23], alkali atoms in vapor cells jump randomly between the hyperfine multiplets of opposite g factors because their thermal kinetic energies are much greater than the hyperfine splitting. All the earlier successes of spin squeezing and entanglement in vapor cells were achieved in low-density vapors with negligible SE rates [29–31]. In the pursuit of larger numbers of squeezed atoms and longer entanglement times, the strong SE coupling regime has attracted more attention recently. Studies include spin entanglements created or preserved by the SE [32–34], the proposal of SE-mediated nuclear spin entangle-ment [35–38], and SE-induced spin noise (SN) correlations between atoms of different alkali species [39–41]. However, the SN of a single alkali species in the strong SE coupling regime has never been precisely studied.

Optical spin noise (OSN) spectroscopy measures the SN-induced Faraday rotation (FR) fluctuations of an off-resonant probe [42–44]. Besides offering a nonperturbative detection of the dynamics of a spin system in thermal or nonthermal states [45–47], OSN also provides a robust tool to calibrate the standard quantum limit and the degree of spin squeezing [48–50]. Note, the OSN is not always proportional to the SN when multiple optical transitions are involved. The dependence of the OSN power on the probe's detuning may be sensitive to spin correlations [51].

This paper studies the OSN spectra of a thermal state alkali vapor in the strong SE coupling regime. We measure the noise spectra in a π-pulse-modulated (πPM) transverse magnetic field [52,53], which shifts the SN resonance out of the swamp of $1/f$ noises whereas acting as an effective zero field for the SE interaction [53]. We eliminate the diffusion distortion of the spectra by letting the probe beam cover the entire cross section of the vapor cell. The cell is antirelaxation coated and contains no buffer gas [54]. As the wall relaxation rate is much lower than the SEC rate, the SE effect dominates the features of the OSN spectra. The absence of buffer gas also causes the optical-transition linewidth to be much smaller than the ground-state hyperfine splitting. Thus, we can probe the atoms without perturbation at smaller detunings and uncover the "polar" frequencies at which the OSN spectrum displays only one of the two types of hyperfine spin correlations.

II. THEORY

We first give a simple theory of the OSN for our system. Assuming the magnetic field points in the x direction and the SE is the only spin interaction, we can write the master

*zhaokf@fudan.edu.cn

equation of the system's density matrix as [4,7]

$$\frac{d\rho}{dt} = \frac{W[\mathbf{I} \cdot \mathbf{S}, \rho]}{i(I + 1/2)} + \frac{\omega_e[S_x, \rho]}{i} + \Gamma[\varphi(1 + 4\langle \mathbf{S} \rangle \cdot \mathbf{S}) - \rho],$$

(1)

where W is the ground-state hyperfine splitting, $\mathbf{S}$ is the electronic spin, $\mathbf{I}$ is the nuclear spin, I is the nuclear spin number, and $\varphi = \rho/4 + \mathbf{S} \cdot \rho \mathbf{S}$ is the nuclear part of ρ, which is not directly affected by the SECs. The SEC rate is $\Gamma = n\sigma v$, where n is the atomic number density, σ is the SEC cross section, and v is the relative speed of atoms. The Larmor frequency of a bare electron is $\omega_e = \gamma_e B$, where γ_e is the gyromagnetic ratio of the electron and B is the magnetic field. Without SECs, the hyperfine spins, $\mathbf{F} \equiv \mathbf{I} + \mathbf{S}$, on the two hyperfine multiplets precess about the field in the opposite sense at the same frequency $\omega_0 = \omega_e/(2I + 1)$.

We will use ^{87}Rb as an example and set $I = 3/2$ hereafter. For a linearly polarized probe beam propagating along the z direction, its FR is $\phi = -nl\Phi$, where l is the cell length, and FR cross-section is $\Phi = \Phi_a + \Phi_b$ [55,56], where

$$\Phi_a(\nu) = \chi_a(\nu) F_{z,a}, \quad \Phi_b(\nu) = \chi_b(\nu) F_{z,b}. \quad (2)$$

The hyperfine spin $F_{z,F}$ is the F_z of the ground-state hyperfine multiplet F, $a = I + 1/2$, $b = I - 1/2$, and $\chi_F(\nu)$ is the detuning factor for multiplet F given by [57]

$$\chi_a(\nu) = \frac{\pi r_e c f_{D1}}{2I + 1} \left[\frac{1}{4} L(\Delta\nu_{aa'}) + \frac{3}{4} L(\Delta\nu_{ab'}) \right],$$

$$\chi_b(\nu) = -\frac{\pi r_e c f_{D1}}{2I + 1} \left[\frac{5}{4} L(\Delta\nu_{ba'}) - \frac{1}{4} L(\Delta\nu_{bb'}) \right], \quad (3)$$

where r_e is the classical radius of the electron, c is the speed of light, $f_{D1} = 0.34$ is the oscillator strength of the ^{87}Rb D1 line, $\Delta\nu_{FF'} \equiv \nu - \nu_{FF'}$ is the detuning from the $F - F'$ resonance, and $L(\Delta\nu_{FF'})$ is the imaginary (dispersive) part of the Voigt profile of the resonance [55]. The OSN is given by the variance of ϕ averaged over all the probed atoms,

$$\overline{\delta^2\phi} = n^2 l^2 \langle \Phi^2 \rangle /nlA_P = \langle \Phi^2 \rangle nl/A_P,, \quad (4)$$

where A_P is the beam area and nlA_P is the total number of atoms being probed simultaneously.

For weak polarizations, Eq. (1) can be linearized. Then we can solve it by treating the Zeeman and SE terms as perturbations to the hyperfine interaction if $W \gg \Gamma, \omega_0$ [4,58]. The Zeeman SN power is nearly independent of ω_0 under the same condition [59].

For weak SE coupling (i.e., $\omega_0 \gg \Gamma_{SE}$), Eq. (1) yields two eigenobservables (EOs) $F_{z,a}$ and $F_{z,b}$ with respective independent decay rates $\gamma_a = \Gamma/8$ and $\gamma_b = 5\Gamma/8$. Thus, the variance of Φ is

$$\langle \Phi^2(\nu) \rangle = \langle \Phi_a^2 \rangle + \langle \Phi_b^2 \rangle = \chi_a^2 \langle F_{z,a}^2 \rangle + \chi_b^2 \langle F_{z,b}^2 \rangle, \quad (5)$$

where the variance of $F_{z,F}$ at the thermal state is given by

$$\langle F_{z,F}^2 \rangle = \frac{2F+1}{2(2I+1)} \frac{F(F+1)}{3} = \begin{cases} 5/4, & F = 2 \\ 1/4, & F = 1. \end{cases} \quad (6)$$

For strong SE coupling (i.e., $\omega_0 = 0$ for simplicity), Eq. (1) yields another pair of independent EOs [4,7],

$$F_{z+} = (F_{z,a} + F_{z,b})/6, \quad F_{z-} = (-F_{z,a} + 5F_{z,b})/6, \quad (7)$$

with respective decay rates $\gamma_+ = 0$, $\gamma_- = 3\Gamma/4$. We have modified the usual eigensolution by replacing the expectation

value of each observable with the observable itself so that we can further calculate their variances. The EO F_{z+} represents a positive hyperfine spin correlation (HSC), which is the weak polarization limit of the well-known spin-temperature state. Conversely, F_{z-} represents a negative HSC wherein the two hyperfine spins orient in opposite directions [4]. With Eq. (7), we can express $F_{z,F}$ in terms of $F_{z\pm}$ in Eq. (2) and obtain $\Phi = \Phi_+ + \Phi_-$, where

$$\Phi_+ = (5\chi_a + \chi_b)F_{z+}, \quad \Phi_- = (-\chi_a + \chi_b)F_{z-}. \quad (8)$$

Using the fact that $\langle F_{z,a}F_{z,b} \rangle = \langle F_{z,a} \rangle_{F=a} \langle F_{z,b} \rangle_{F=b} = 0$ at the thermal state, we get $\langle F_{z+}F_{z-} \rangle = 0$ and $\langle \Phi_+\Phi_- \rangle = 0$. Therefore, the total variance of Φ in a zero field is

$$\langle \Phi^2 \rangle_{ZF} = \langle \Phi_+^2 \rangle + \langle \Phi_-^2 \rangle,$$

$$\langle \Phi_+^2 \rangle = \frac{(5\chi_a + \chi_b)^2}{36} [\langle F_{z,a}^2 \rangle + \langle F_{z,b}^2 \rangle], \quad (9)$$

$$\langle \Phi_-^2 \rangle = \frac{(\chi_a - \chi_b)^2}{36} [\langle F_{z,a}^2 \rangle + 25\langle F_{z,b}^2 \rangle].$$

Such HSCs of noise in a single alkali vapor are similar to the SN cross correlations of different species in a mixed vapor [40]. Although Eqs. (9) and (5) look different, after inserting the values of $\langle F_{z,F}^2 \rangle$ from Eq. (6), we obtain

$$\langle \Phi^2(\nu) \rangle_{ZF} = \langle \Phi^2(\nu) \rangle = (5\chi_a^2 + \chi_b^2)/4. \quad (10)$$

This means that the total OSN power is independent of the SE coupling strength. To compare with the experimental results, we define the following power ratios:

$$\xi_\pm(\nu) \equiv \langle \Phi_\pm^2(\nu) \rangle / \langle \Phi^2(\nu) \rangle,$$

$$\xi \equiv \langle \Phi^2(\nu) \rangle_{ZF} / \langle \Phi^2(\nu) \rangle = \xi_+ + \xi_-. \quad (11)$$

Although $\xi = 1$ according to Eq. (10), $\xi_+(\nu)$ and $\xi_-(\nu)$ vary complementarily between 0 and 1 with the detuning. At two polar frequencies $\nu_\pm$ defined by $\chi_a(\nu_+) = \chi_b(\nu_+)$, $5\chi_a(\nu_-) = -\chi_b(\nu_-)$, we have $\xi_\pm(\nu_\pm) = 1$. Namely, the zero-field OSN is Φ_+ or Φ_- polarized respectively. For the case of far detunings (i.e., $|\Delta\nu_{FF'}| \gg W$), $\chi_b \approx -\chi_a$. Thus, we have $\xi_+(\infty) = 4/9$ and $\xi_-(\infty) = 5/9$. For an arbitrary alkali species, we find that the power ratio of the negative to the positive HSC component is given by

$$\frac{\langle \Phi_-^2(\infty) \rangle}{\langle \Phi_+^2(\infty) \rangle} = \frac{\xi_-}{\xi_+} = \frac{([I]^2 - 1)([I]^2 - 4)}{9[I]^2}, \quad (12)$$

where $[I] \equiv 2I + 1$. This ratio is greater than 1 for $I > 1$.

Finally, based on the fluctuation-dissipation theorem [60], the autocorrelation function of Φ in a zero field is as follows:

$$C(\tau) = (\langle \Phi_+^2 \rangle e^{-\gamma_+\tau} + \langle \Phi_-^2 \rangle e^{-\gamma_-\tau})e^{-\gamma_W\tau}, \quad (13)$$

where the last factor is added to roughly describe other weak relaxations neglected in the master equation. The power spectral density (PSD) of Φ is $C(\tau)$'s Fourier transform.

III. EXPERIMENTAL RESULTS

Our experimental setup is shown in Fig. 1. A fused quartz vapor cell internally coated with an antirelaxation film of octadecyltrichlorosilane [61] is filled with enriched ^{87}Rb. The cell is 23-mm long and 8×8 mm^2 in the cross section. It
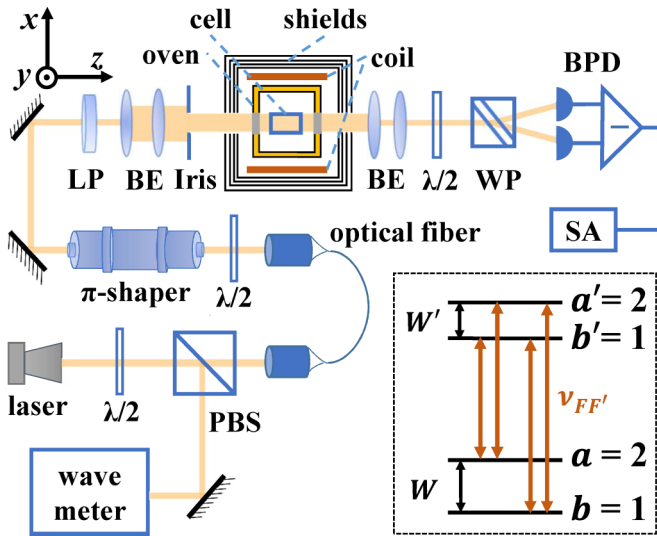
FIG. 1. Experimental setup. Polarizing beam splitter (PBS); $\lambda/2$, half-wave plate; π shaper, Gaussian to flattop beam profile convertor; linear polarizer (LP); beam expander (BE); Iris, adjustable rectangular aperture; Wollaston prism (WP); balanced photodetector (BPD); spectrum analyzer (SA). The inset is the hyperfine structure of the ^{87}Rb $D1$ line. The ground- and the excited-state hyperfine splittings are $W = 6.8$ and $W' = 0.8$ GHz, respectively.

FIG. 2. The OSN spectra in a DC field and a πPM field. The cell's stem temperature $T = 108.2\,°\mathrm{C}$; the probe's power is 0.19 mW; the probe is red-detuned 14.1 GHz from the ab' transition. The data averaged for 320 s (black circle) are fitted by the theory (solid red line). The frequency resolutions of the DC field spectrum and πPM-field spectrum are 16 Hz and 1 Hz respectively. The πPM-field spectrum is scanned about its first SN harmonic when the transverse field is being pulse-modulated at 2 kHz with 0.14% duty cycle.

sits in a ceramic oven wrapped and heated by a nonmagnetic wire passing an AC of 71 kHz. The cell's stem is kept a few degrees cooler than the body. A set of Helmholtz coils driven by a low noise current source (ADC6156) produces a DC magnetic-field $\mathbf{B}_0$ in the x direction. Another set of coils driven by a homemade pulse-current source creates a pulse-modulated-field $\mathbf{B}_p$ along the same axis. The whole setup is contained in a four-layer μ-metal shield. We probe the OSN with a diode laser (Toptica DLpro), which can be detuned between ± 60 GHz about the ^{87}Rb $D1$ line and is monitored by a wavemeter (Bristol 771B). We convert the beam profile to a flattop square to match the cell's cross section using a single-mode optical fiber, a π Shaper, a beam expander, and a rectangular iris. The probe's initial plane of polarization is set at the magic angle (i.e., 54.7° to $\mathbf{B}_0$) to eliminate any tensor light shift [62,63]. A Wollaston prism and a balanced photodetector behind the cell measure the probe's FR. An SRS760 SA produces the PSD of the FR signal with averaging times from 5 to 30 min depending on the signal size. The final OSN is obtained by subtracting the background PSD measured at $B_0 = 0.5$ G in which the SN resonances are outside the SA's bandwidth.

To understand the experiment data, we review the property of SN spectra in a πPM field with modulation rate ν_p and duty cycle d [53]. The spectrum contains a series of equal-width resonant harmonics peaked at odd integer (n_p) multiples of $\nu_p/2$ with amplitude $\propto 1/n_p^2$. The total SN power equals the power of the first harmonic $(n_p = 1)$ divided by $\pi^2/8 \approx 0.81$. Since a πPM-field is equivalent to a zero field for isotropic spin interactions, the SE broadening drops to d times its value in a large DC field.

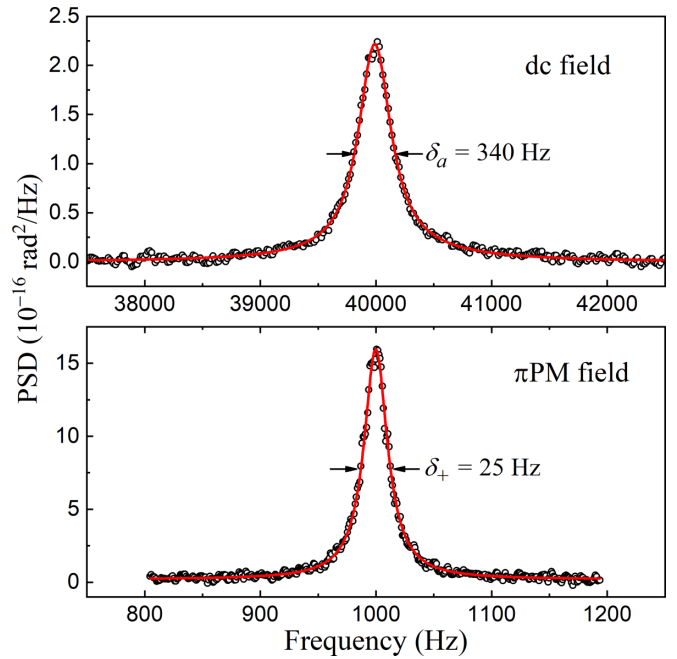In Fig. 2, we compare the OSN spectra measured in a DC field and a πPM field corresponding to the weak and

strong SE coupling regimes, respectively. We fit the DC-field spectrum by the sum of two Lorentzian resonances of the uncorrelated hyperfine spin noises, i.e., $\langle\Phi_a^2\rangle$ and $\langle\Phi_b^2\rangle$. Their center frequencies are set 159 Hz apart in the fitting to account for the nuclear spin Zeeman effect. The full width of the $\langle\Phi_a^2\rangle$ peak is $\delta_a = \delta_w + \gamma_a/\pi$, where δ_w is the wall relaxation broadening. The total fitted area gives the value of $\langle\Phi^2\rangle$. For the πPM-field spectrum, we fit the first harmonic by a single Lorentzian. The fitted area divided by 0.81 gives the value of $\langle\Phi_+^2\rangle$. The 25-Hz fitted linewidth is mostly given by δ_w as the SE broadening is less than $\delta_a d \sim 0.5$ Hz in the πPM field. With δ_a and δ_w, we have $\gamma_a/\pi \approx 315$ Hz. In Fig. 2, we rescanned the πPM-field spectrum of Fig. 3 with a wider frequency range. We can now see the first three harmonics of the SN. The enlarged base of the spectrum reveals the broad negative HSC component, which can be fitted by the sum of three Lorentzians obeying the properties of πPM-field spectra described earlier. The fitted area of the first harmonic divided by 0.81 gives $\langle\Phi_-^2\rangle$. The fitted full width is 1.6 kHz, which is $\sim \gamma_-/\pi$. On the other hand, using the measured value of γ_a and the relation between γ_- and γ_a, we have $\gamma_-/\pi = 6\gamma_a/\pi = 1.9$ kHz. This small discrepancy might be due to the blending of the $\langle\Phi_+^2\rangle$ peak into the $\langle\Phi_-^2\rangle$ peak.

From Figs. 2 and 3, we get $\xi_+ = 0.58(3)$ and $\xi = 1.01(6)$. We find no systematic dependence of ξ_+ on the probe power from 0.08 to 1.8 mW within 9% uncertainty. In Fig. 4(a), we plot the dependence of ξ_+ and ξ on the probe's detuning
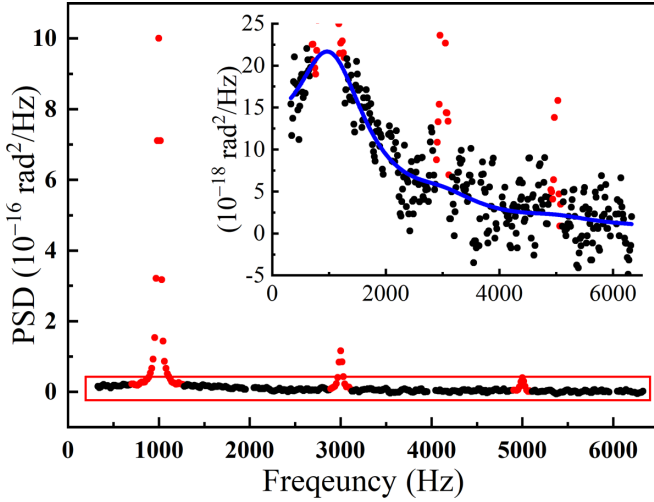
FIG. 3. A wider scan of the πPM-field OSN spectrum at the same condition as Fig. 2 shows two more peaks of SN harmonics. Since the SA can plot only 400 points, the resolution of this scan is 15.6 Hz, close to the linewidth of each peak, which makes the first peak lower than the one in Fig. 2. The inset zooms in on the bottom part of the spectrum. The blue line is the fit for the broad negative HSC component (black points). Note, the electronic interference spikes at integer multiples of the pulse-modulation rate have been trimmed.

relative to the $D1$ transition frequency without hyperfine splitting. The experimental results agree with the numerical calculation of the theory very well. The detunings of the polar frequencies ν_+ and ν_- are found to be 0.6 and 6.3 GHz, where ξ_+ is 1 and 0, respectively. The OSN at ν_- is shown in Fig. 4(b), and only the $\langle \Phi_-^2 \rangle$ component is visible.

IV. DISCUSSIONS AND CONCLUSIONS

To summarize, we study the zero-field OSN spectra of a dense alkali vapor at thermal equilibrium. In this strong SE coupling regime or the SERF regime, the spectrum consists of two components corresponding to a positive and a negative HSC. Their power percentages relative to the total noise vary complementarily between 0 and 1 with the probe's detuning frequency. There are two polar frequencies at which the OSN spectrum is 100% polarized with only one HSC component. The other HSC component still exists in the spin system, but it is invisible to the FR probe. Thus, these polar frequencies allow the probe to interact selectively with one of the HSC components and provide special channels on the light-atom quantum interface. At the far-detuning limit, the most common condition of FR detection, the negative HSC component contains more than half of the total OSN power. However, its spectral profile is much lower and wider than that of the positive one. Overlooking its contribution either by low-pass filtering the FR signal or fitting the OSN spectrum with a single Lorentzian will yield a smaller power of the total SN. In the time domain, a random spin fluctuation will quickly relax into the relatively long-lived spin temperature state by dissipating its negative HSC component. Such effects will be distinguished from spin squeezing. Since the strength and duration of each SEC and the period of hyperfine interaction
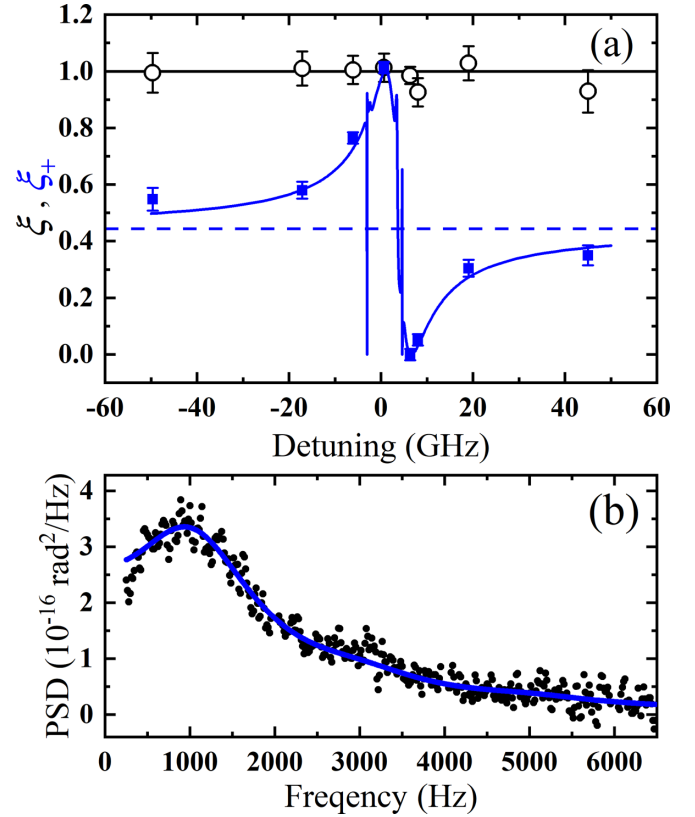

FIG. 4. (a) The detuning dependence of ξ_+ and ξ at $T = 108.2$ °C. For ξ_+: experiment (blue square) and theory (solid blue line). The dashed blue line is the far-detuning limit $\xi_+(\infty)$. For ξ: experiment (black circle) and theory (horizontal solid black line). (b) The PSD measured at 6.3 GHz detuning, i.e., ν_-. The spectrum contains only the $\langle \Phi_-^2 \rangle$ peak, and its fitting returns a full width of 1.9 kHz.

between two successive SECs depend on the thermal kinetic motions of the atoms, all the quantum phase correlations seem to be randomized. However, the conservation of spin angular momentum for the SE or the hyperfine interaction preserves certain order in the system, such as the population correlation of a spin temperature state, the integrity of a stretched state, and the entanglement of a macroscopic singlet state [33]. It is unclear whether some other entangled states can also live long in the strong SE coupling regime.

As a last note, our method of deriving the OSN spectrum using the eigensolution of the density-matrix equation can also apply to other types of spin interactions and systems of multiple species. Thus, much knowledge from the previous works [4,7,58,64] can be readily used.

[1] J. P. Wittke and R. H. Dicke, Phys. Rev. **103**, 620 (1956).

[2] E. M. Purcell and G. B. Field, Astrophys. J. **124**, 542 (1956).

[3] F. Grossetete, J. Phys. **25**, 383 (1964).

[4] W. Happer and A. C. Tam, Phys. Rev. A **16**, 1877 (1977).

[5] M. A. Bouchiat, T. R. Carver, and C. M. Varnum, Phys. Rev. Lett. **5**, 373 (1960).

[6] T. G. Walker and W. Happer, Rev. Mod. Phys. **69**, 629 (1997).

[7] S. Appelt, A. Ben-Amar Baranga, C. J. Erickson, M. Romalis, A. R. Young, and W. Happer, Phys. Rev. A **58**, 1412 (1998).

[8] T. R. Gentile, P. J. Nacher, B. Saam, and T. G. Walker, Rev. Mod. Phys. **89**, 045004 (2017).

[9] D. Budker and M. Romalis, Nat. Phys. **3**, 227 (2007).

[10] J. Vanier and C. Audoin, *The Quantum Physics of Atomic Frequency Standards*, Vol. 1 (Institute of Physics Publishing, 1989).

[11] M. S. Albert, G. D. Cates, B. Driehuys, W. Happer, B. Saam, C. S. Springer Jr., and A. Wishnia, Nature (London) **370**, 199 (1994).

[12] K. Ruppert, Rep. Prog. Phys. **77**, 116701 (2014).

[13] B. C. Grover, Phys. Rev. Lett. **40**, 391 (1978).

[14] M. A. Rosenberry and T. E. Chupp, Phys. Rev. Lett. **86**, 22 (2001).

[15] W. Happer and H. Tang, Phys. Rev. Lett. **31**, 273 (1973).

[16] J. C. Allred, R. N. Lyman, T. W. Kornack, and M. V. Romalis, Phys. Rev. Lett. **89**, 130801 (2002).

[17] I. K. Kominis, T. W. Kornack, J. C. Allred, and M. V. Romalis, Nature (London) **422**, 596 (2003).

[18] T. W. Kornack and M. V. Romalis, Phys. Rev. Lett. **89**, 253002 (2002).

[19] T. W. Kornack, R. K. Ghosh, and M. V. Romalis, Phys. Rev. Lett. **95**, 230801 (2005).

[20] G. Vasilakis, J. M. Brown, T. W. Kornack, and M. V. Romalis, Phys. Rev. Lett. **103**, 261801 (2009).

[21] M. Smiciklas, J. M. Brown, L. W. Cheuk, S. J. Smullin, and M. V. Romalis, Phys. Rev. Lett. **107**, 171604 (2011).

[22] J. Lee, A. Almasi, and M. Romalis, Phys. Rev. Lett. **120**, 161801 (2018).

[23] T. L. Ho, Phys. Rev. Lett. **81**, 742 (1998).

[24] T. Ohmi and K. Machida, J. Phys. Soc. Jpn. **67**, 1822 (1998).

[25] E. M. Bookjans, C. D. Hamley, and M. S. Chapman, Phys. Rev. Lett. **107**, 210406 (2011).

[26] X.-Y. Luo, Y.-Q. Zou, L.-N. Wu, Q. Liu, M.-F. Han, M. K. Tey, and L. You, Science **355**, 620 (2017).

[27] Y.-Q. Zou, L.-N. Wu, Q. Liu, X.-Y. Luo, S.-F. Guo, J.-H. Cao, M. K. Tey, and L. You, Proc. Natl. Acad. Sci. USA **115**, 6381 (2018).

[28] L. Pezze, A. Smerzi, M. K. Oberthaler, R. Schmied, and P. Treutlein, Rev. Mod. Phys. **90**, 035005 (2018).

[29] B. Julsgaard, A. Kozhekin, and E. S. Polzik, Nature **413**, 400 (2001).

[30] G. Vasilakis, H. Shen, K. Jensen, M. Balabas, D. Salart, B. Chen, and E. S. Polzik, Nat. Phys. **11**, 389 (2015).

[31] H. Bao, J. Duan, S. Jin, X. Lu, P. Li, W. Qu, M. Wang, I. Novikova, E. E. Mikhailov, K.-F. Zhao, K. Mølmer, H. Shen, and Y. Xiao, Nature (London) **581**, 159 (2020).

[32] I. K. Kominis, Phys. Rev. Lett. **100**, 073002 (2008).

[33] J. Kong, R. Jiménez-Martínez, C. Troullinou, V. G. Lucivero, G. Tóth, and M. W. Mitchell, Nat. Commun. **11**, 2415 (2020). Although SECs conserve the macroscopic singlet state in theory, this work has not considered the negative HSC of the spin

noise, which might affect its final estimate of the degree of spin squeezing.

[34] K. Mouloudakis and I. K. Kominis, Phys. Rev. A **103**, L010401 (2021).

[35] A. Dantan, G. Reinaudi, A. Sinatra, F. Laloë, E. Giacobino, and M. Pinard, Phys. Rev. Lett. **95**, 123002 (2005).

[36] O. Katz, R. Shaham, E. S. Polzik, and O. Firstenberg, Phys. Rev. Lett. **124**, 043602 (2020).

[37] O. Katz, R. Shaham, and O. Firstenberg, arXiv:1905.12532.

[38] R. Shaham, O. Katz, and O. Firstenberg, arXiv:2102.02797.

[39] A. T. Dellis, M. Loulakis, and I. K. Kominis, Phys. Rev. A **90**, 032705 (2014).

[40] D. Roy, L. Y. Yang, S. A. Crooker, and N. A. Sinitsyn, Sci. Rep. **5**, 9573 (2015).

[41] K. Mouloudakis, M. Loulakis, and I. K. Kominis, Phys. Rev. Res. **1**, 033017 (2019).

[42] E. B. Aleksandrov and V. S. Zapassky, Zh. Eksp. Teor. Fiz. **81**, 132 (1981) .

[43] V. S. Zapasskii, Adv. Opt. Photonics **5**, 131 (2013).

[44] N. A. Sinitsyn and Y. V. Pershin, Rep. Prog. Phys. **79**, 106501 (2016).

[45] S. A. Crooker, D. G. Rickel, A. V. Balatsky, and D. L. Smith, Nature (London) **431**, 49 (2004).

[46] F. X. Li, Y. V. Pershin, V. A. Slipko, and N. A. Sinitsyn, Phys. Rev. Lett. **111**, 067201 (2013).

[47] P. Glasenapp, N. A. Sinitsyn, L. Y. Yang, D. G. Rickel, D. Roy, A. Greilich, M. Bayer, and S. A. Crooker, Phys. Rev. Lett. **113**, 156601 (2014).

[48] J. L. Sorensen, J. Hald, and E. S. Polzik, Phys. Rev. Lett. **80**, 3487 (1998).

[49] A. Kuzmich, L. Mandel, and N. P. Bigelow, Phys. Rev. Lett. **85**, 1594 (2000).

[50] G. Vasilakis, V. Shah, and M. V. Romalis, Phys. Rev. Lett. **106**, 143601 (2011).

[51] V. S. Zapasskii, A. Greilich, S. A. Crooker, Y. Li, G. G. Kozlov, D. R. Yakovlev, D. Reuter, A. D. Wieck, and M. Bayer, Phys. Rev. Lett. **110**, 176601 (2013).

[52] M. E. Limes, D. Sheng, and M. V. Romalis, Phys. Rev. Lett. **120**, 033401 (2018).

[53] G. Zhang, Y. Wen, J. Qiu, and K. Zhao, Opt. Express **28**, 15925 (2020).

[54] Y. Tang, Y. Wen, L. Cai, and K. Zhao, Phys. Rev. A **101**, 013821 (2020).

[55] S. J. Seltzer, Ph.D. Thesis, Princeton University Press, Princeton (2008).

[56] V. Shah, G. Vasilakis, and M. V. Romalis, Phys. Rev. Lett. **104**, 013601 (2010).

[57] W. Happer and B. S. Mathur, Phys. Rev. **163**, 12 (1967).

[58] W. Happer, Rev. Mod. Phys. **44**, 169 (1972).

[59] B. Mihaila, S. A. Crooker, D. G. Rickel, K. B. Blagoev, P. B. Littlewood, and D. L. Smith, Phys. Rev. A **74**, 043819 (2006).

[60] R. Kubo, Rep. Prog. Phys. **29**, 255 (1966).

[61] G. Zhang, L. Wei, M. Wang, and K. Zhao, J. Appl. Phys. **117**, 043106 (2015).

[62] B. S. Mathur, H. Tang, and W. Happer, Phys. Rev. **171**, 11 (1968).

[63] W. Chalupczak and R. M. Godun, Phys. Rev. A **83**, 032512 (2011).

[64] O. Katz, O. Peleg, and O. Firstenberg, Phys. Rev. Lett. **115**, 113003 (2015).